microbiology research

MDPI

Brief Report

Functional Characterization of CfRgs2 Reveals Its Critical Role in Growth, Conidiation, Stress Response, and Virulence of *Colletotrichum fructicola*

Yadi Liu, Qiuyue Hu and He Li *

Key Laboratory of Forest Bio-resources and Integrated Pest Management for Higher Education in Hunan Province, Central South University of Forestry and Technology, Changsha 410004, China; t20060695@csuft.edu.cn (Y.L.)
* Correspondence: t20061078@csuft.edu.cn

Abstract

Colletotrichum fructicola is the predominant pathogenic agent responsible for anthracnose in *Camellia oleifera*. RGS2 is a GTPase-activating protein that negatively regulates G-protein signaling by inactivating Gα subunits. In this study, we characterized the ortholog of *CfRGS2* in *C. fructicola* to explore its pathogenic roles. Seven canonical *RGS* genes were identified through BLASTp and keyword searches. Conserved domains and subcellular localizations were predicted bioinformatically. A *CfRGS2* knockout mutant was generated via overlap-PCR and PEG-mediated transformation, verified by PCR, and complemented by reintroducing the wild-type gene. Phenotypic characterization showed that the growth rates of mutants Δ*Cfrgs2*-1 and Δ*Cfrgs2*-2 were significantly reduced compared with those of the wild-type and complemented strains. On both PDA and minimal medium, the mutant strains exhibited significantly smaller colony diameters of 3.3 cm and 3.1 cm, respectively, relative to the control strains. Moreover, conidiation in the mutants was only 4% of that in the wild-type and complemented strains, and appressorium formation was reduced to 6%, with statistical analyses confirming high significance. Under cell wall stress induced by 400 μg/mL Congo red, the growth inhibition rates of Δ*Cfrgs2*-1 and Δ*Cfrgs2*-2 were 44% and 48%, respectively, significantly higher than those of the control strains. Pathogenicity assays demonstrated that the mutants failed to induce lesions on unwounded leaves and caused 47% and 30% smaller lesion areas on wounded apple fruits, respectively. In summary, *C. fructicola* possesses seven canonical RGS proteins that regulate G-protein signaling, among which CfRgs2 is implicated in growth, conidiation, the stress response to cell wall perturbation, and virulence.

Keywords: *Camellia oleifera* anthracnose; *Colletotrichum fructicola*; G-protein signaling regulator; *CfRGS2*; pathogenicity

Academic Editors: Thanyani Emelton Ramadwa and Stephen Meddows-Taylor

Received: 28 January 2026
Revised: 27 February 2026
Accepted: 28 February 2026
Published: 2 March 2026

1. Introduction

Camellia oleifera is the most widely cultivated and economically valuable woody oil crop in China, holding a strategic role in ensuring national edible oil security and driving economic development in mountainous regions. However, the industry is severely constrained by the persistent anthracnose epidemic, which causes flower and fruit drop and results in substantial economic losses. Previous pathogenicity studies have established *Colletotrichum fructicola* as the predominant causal agent of this disease [1]. Nevertheless, the molecular mechanisms underlying *C. fructicola*'s pathogenicity and its interaction with

the host plant remain elusive. This study, therefore, aims to unravel these key pathogenic mechanisms, providing a theoretical foundation for novel control strategies.

The heterotrimeric G-protein signaling pathway is a canonical pathway in eukaryotic cells for perceiving and transducing extracellular signals. It regulates critical fungal processes, including growth, development, reproduction, mating, host invasion, and pathogenicity [2,3]. G-proteins are activated by G protein-coupled receptors (GPCRs). Ligand binding to a GPCR triggers the exchange of GDP for GTP on the Gα subunit, inducing a conformational change in the heterotrimer that leads to the dissociation of Gα from the Gβγ dimer [4,5]. Regulators of G-protein signaling (RGS) serve as key negative regulators of this pathway. They function as GTPase-activating proteins (GAPs) for the Gα subunit, accelerating the hydrolysis of GTP to GDP. This inactivates the Gα subunit, promotes the re-association of the heterotrimer, and rapidly terminates G-protein signaling [6,7].

The RGS domain constitutes the catalytic core essential for the GTPase-activating function of RGS proteins; its deletion or disruption completely abolishes GAP activity [8]. The functional significance of RGS proteins has been established in a range of plant-pathogenic fungi, including *Magnaporthe oryzae* and *Gibberella zeae*. These studies position RGS proteins as pleiotropic regulators of fundamental biology, governing processes from vegetative growth and sporulation to sexual reproduction, secondary metabolism (including toxin and pigment production), and virulence [6,9,10].

In *S. cerevisiae*, RGS2 acts as a negative regulator of glucose-induced cAMP signaling by directly activating the Gpa2 protein within the G-protein pathway, thereby modulating the amplitude of cAMP accumulation [11]. In contrast, the function of the RGS2 ortholog in *C. fructicola* remains uncharacterized. Here, we identified putative RGS homologs in *C. fructicola* by querying its protein database with the four canonical RGS amino acid sequences from *S. cerevisiae* S288c, supplemented by keyword searches. The identity and number of RGS proteins in this pathogen were confirmed through bioinformatic analyses, including conserved-domain prediction and subcellular localization analysis. Furthermore, we employed a reverse genetics approach to generate a targeted knockout of the *CfRGS2* gene and elucidate its biological function. This study aims to define the role of *CfRGS2*, which may serve as a potential target for the development of novel, green-targeted fungicides.

2. Materials and Methods

2.1. Strains

The wild-type (WT) strain CFLH16 of *C. fructicola* was previously isolated, identified, and maintained in our laboratory [12]. The Δ*Cfrgs2* mutant and the complemented strain Δ*Cfrgs2/CfRGS2* were generated in this study.

2.2. Identification of Rgs Proteins, Prediction of Conserved Domains, and Subcellular Localization Analysis

Based on the amino acid sequences of the four Rgs proteins (Sst2, Rgs2, Rax1, and Mdm1) from *Saccharomyces cerevisiae* S288c, a BLASTp (BLAST version 2.14.0+) search was performed against the *C. fructicola* protein database using default parameters to identify canonical RGS proteins [13]. Additionally, the database was queried using the keywords "Regulators of G-protein signaling" and "RGS" to retrieve relevant sequences. The accession numbers of the identified RGS proteins in *C. fructicola* were confirmed via NCBI (http://www.ncbi.nlm.nih.gov, accessed on 8 January 2026). The conserved domains of these RGS proteins were analyzed using the SMART online platform (http://smart.embl-heidelberg.de/, accessed on 8 January 2026), and their subcellular localization was predicted using ProtComp v9.0.

2.3. Phylogenetic Analysis

To elucidate the biological function of the Rgs2 protein in *C. fructicola*, a homologous Rgs2 sequence was retrieved by performing a BLASTp search against the *C. fructicola* protein database, using the sequence of the regulator of G-protein signaling 2 (Rgs2; NP_014750.3) from *Saccharomyces cerevisiae* as the query. Subsequently, a neighbor-joining (N-J) phylogenetic tree was constructed with MEGA 7.0 software using the homologous Rgs2 amino acid sequences from *C. fructicola*, *C. gloeosporioides*, *Verticillium longisporum*, *M. oryzae*, and *Saccharomyces cerevisiae*.

2.4. Gene Knockout and Mutant Verification

The procedures for gene knockout, PCR amplification, plasmid isolation, fungal transformation, transformant selection, and conidiation quantification were carried out following previously described methods [12,14]. Briefly, the upstream flank, downstream flank, and the hygromycin phosphotransferase (*HPH*) cassette were amplified by PCR using primer pairs 1F/2R, 3F/4R, and Hyg-F/Hyg-R, respectively. These three fragments were then fused via fusion PCR with the outer primers 1F/4R to generate the final *CfRGS2* knockout cassette. Putative knockout mutants were initially screened by PCR. Successful gene deletion was confirmed by the absence of a PCR product using the gene-internal primer pair 7F/8R, and the presence of a product using the flanking primer pair 5F/H885R. The mutants were further verified by quantitative PCR (qPCR). All primers used in this study are listed in Table 1.

Table 1. Primer used in this study.

Primer Name	Primer Sequences (5′-3′)	Purpose
1F	AGCGATCAAGACGTCACATC	Amplify the *CfRGS2* 5′ flank sequence
2R	TTGACCTCCACTAGCTCCAGCCAAGCCGACTATGTTGG TTTCCCAGC	Amplify the *CfRGS2* 5′ flank sequence
3F	CAAAGGAATAGAGTAGATGCCGACCGCGCGCCATCAT TACAACGTT	Amplify the *CfRGS2* 3′ flank sequence
4R	GCCAACTCGTTGGAGTACAA	Amplify the *CfRGS2* 3′ flank sequence
5F	CTGTTGCATAACCACACCCA	Validation of the *CfRGS2* gene deletion
H855R	GCTGATCTGACCAGTTGC	Validation of the *CfRGS2* gene deletion
Hyg-F	GGCTTGGCTGGAGCTAGTGGAGGTCAA	Amplify the HPH sequence
Hyg-R	CGGTCGGCATCTACTCTATTCCTTTG	Amplify the HPH sequence
7F	TGTCACGCCACCTTCACTTT	Amplify the *CfRGS2* gene sequence
8R	CAGCACTTCCACTGTCGTCT	Amplify the *CfRGS2* gene sequence
9F	ACTCACTATAGGGCGAATTGGGTACTCAAATTGGTTAG CAAGTACGGATACCTGGA	Amplify the complemented sequence
10R	CACCACCCCGGTGAACAGCTCCTCGCCCTTGCTCACAC TAGAGGTGCTGCTTGCGC	Amplify the complemented sequence
GFPR	GACACGCTGAACTTGTGGCCGTT	Validation of the complemented sequence

2.5. Complementation Assay

The complementation plasmid was constructed according to the methodology described by Gao et al. [14]. A DNA fragment containing the *CfRGS2* gene and its native promoter was amplified by PCR using the primers 9F/10R. This fragment was subsequently co-transformed with the linearized pYF11 vector into the yeast strain XK-125 for in vivo assembly via homologous recombination, resulting in the construction of the pYF11::*CfRGS2* plasmid. The assembled plasmid was initially confirmed by PCR with primers CfRgs2-7F/GFPR, then extracted and introduced into *E. coli* DH5α(Beijing Tsingke Biotech Co., Ltd., Beijing, China) competent cells for propagation. Plasmid DNA isolated from positive *E. coli* clones was subjected to further PCR verification and sequencing. The sequence-verified plasmid was finally transformed into Δ*Cfrgs2* protoplasts. Transformants were selected

based on bleomycin resistance and subsequently screened for GFP fluorescence, yielding the complemented strain *Cfrgs2/CfRGS2*.

2.6. Vegetative Growth Assay

Mycelial plugs of identical diameter from the actively growing margin of each strain (WT, Δ*Cfrgs2*, and Δ*Cfrgs2/CfRGS2*) were inoculated onto potato dextrose agar (PDA) and minimal medium (MM) plates. Following incubation at 28 °C for 3 days, the colony diameters were measured to assess radial growth.

2.7. Cell Wall Stress Tolerance Assay

To evaluate the role of *CfRGS2* in cell wall stress response, mycelial plugs of the same strains were placed onto PDA medium supplemented with 400 μg/mL Congo Red (Beijing Solarbio Science & Technology Co., Ltd., Beijing, China). After a 3-day incubation at 28 °C, colony growth was recorded to determine the growth inhibition rate relative to the control.

2.8. Conidiation and Appressorium Formation Assay

Mycelial plugs (WT, Δ*Cfrgs2*, and Δ*Cfrgs2/CfRGS2*) of identical diameter were cultured in potato dextrose broth at 28 °C with agitation (180 rpm) for 3 days. Conidial yields were determined by direct counting using a hemocytometer. To assay appressorium formation, conidia from these cultures were filtered, washed, and diluted to a final concentration of 1×10^5 conidia/mL. Aliquots (10 μL) of each spore suspension were then applied to the surface of sterile hydrophobic coverslips and incubated under high humidity at 28 °C in the dark. The percentage of germinated conidia forming appressoria was quantified after 12 h.

2.9. Pathogenicity Assays

The WT, Δ*Cfrgs2*, and complemented Δ*Cfrgs2/CfRGS2* strains were point-inoculated at the margins of healthy *C. oleifera* leaves and maintained under humid conditions at 28 °C for 3 days. Lesion development was subsequently documented and quantified. In parallel, the same set of strains was inoculated onto wounded apple fruits (Fuji), following the methodology outlined in our previous study [15]. After a 3-day incubation period, lesion diameters were measured and subjected to statistical analysis.

2.10. Statistical Analysis

Each result was shown as the mean ± SD of three replicates. The significance of differences between samples was analyzed using ANOVA (Analysis of Variance) with Duncan's new multiple-range test. The level of significance was set at $p < 0.01$.

3. Results

3.1. Identification and Characterization of RGS Proteins in C. fructicola

Bioinformatic analysis identified seven putative RGS proteins in *C. fructicola*. The initial identification was performed by conducting a BLAST-p search against the *C. fructicola* protein database, using the amino acid sequences of the four canonical RGS proteins from *S. cerevisiae*—Sst2, Rgs2, Rax1, and Mdm1. This approach revealed four homologs: a sequence (KAF4488684.1) homologous to Sst2 was designated CfRgs1; a sequence (XP_031882679.1) homologous to Rgs2 was designated CfRgs2; a sequence (XP_031890408.1) homologous to Rax1 was designated CfRgs3; and a sequence (XP_031890755.1) homologous to Mdm1 was designated CfRgs4. A subsequent search using the keywords "Regulator of G-protein signaling" and "RGS" yielded three additional sequences (XP_031885571.1, XP_031878127.1, and XP_031889684.1). Based on their domain characteristics, these were designated CfRgs5, CfRgs6, and CfRgs7, respectively (Table 2).

Table 2. The subcellular localization of Rgs in *C. fructicola*.

Name	Nuclear	Plasma Membrane	Extracellular	Cytoplasmic	Mitochondrial	Endoplasmic Reticulum	Peroxisomal	Lysosomal	Golgi	Acuolar	Accession Number
CfRGS1	1.87	2.11	0	2.54	1.96	0.32	0.81	0	0	0.39	KAF4488684.1
CfRGS2	3.84	1.68	1.49	0.66	1.36	0	0.33	0	0.64	0	XP_031882679.1
CfRGS3	0.49	3.55	0.52	0.56	2.47	0.67	0	0.31	1.07	0.35	XP_031890408.1
CfRGS4	8.47	0	0.01	0.02	0	0	0	0	1.45	0.05	XP_031890755.1
CfRGS5	4.21	1.54	0.88	0.64	1.97	0.08	0.36	0	0.31	0	XP_031885571.1
CfRGS6	0.35	5.06	1.31	0.36	1.75	0.34	0.12	0.08	0.53	0.10	XP_031878127.1
CfRGS7	0.21	1.49	0	0.02	0.32	7.96	0	0	0	0	XP_031889684.1

Footnote: Subcellular localization was predicted using ProtComp v9.0 (Softberry) for eukaryotic fungi. Integral scores (0–10) indicate prediction confidence, with higher scores representing greater reliability. The localization with the highest score was considered the most probable for each protein.

Domain architecture analysis of all seven proteins using the SMART online tool confirmed that each possesses the canonical RGS domain. In addition, these proteins contain various auxiliary domains, including DEP, PAC, PX, and PXA (Figure 1). This domain composition is similar to that reported for RGS proteins in *M. oryzae* [10].

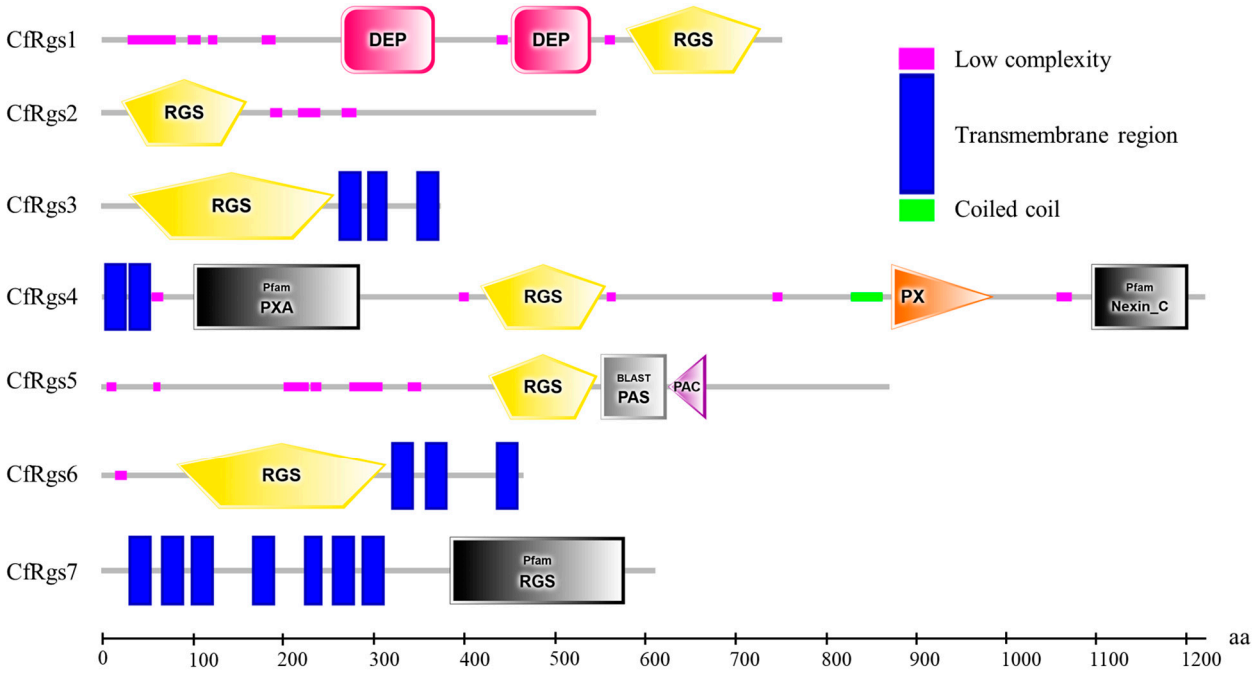

Figure 1. The conserved domain of seven RGS in *Colletotrichum fructicola.* Note: RGS: Regulator of G protein signaling domain; DEP: Domain found in Disheveled, Egl-10, and Pleckstrin; PAC: Motif C-terminal to PAS motifs; PX: PhoX homologous domain.

3.2. Subcellular Localization Prediction

Subcellular localization of the seven identified RGS proteins in *C. fructicola* was predicted using TMHMM. The analysis indicated distinct localization patterns for each protein. Specifically, CfRgs1 was primarily predicted to localize to the nucleus, plasma membrane, and cytoplasm, suggesting it may function as a nucleocytoplasmic shuttling protein. CfRgs2, CfRgs4, and CfRgs5 were predicted to be nuclear-localized. In contrast, CfRgs3 and CfRgs6 were associated with the plasma membrane, while CfRgs7 was predicted to reside in the endoplasmic reticulum (Table 2).

3.3. Phylogenetic Analysis of CfRgs2

To confirm the orthology of the identified RGS proteins in *C. fructicola*, we performed a phylogenetic analysis with RGS proteins from other well-studied fungi. The *CfRGS2* gene comprises 1782 base pairs, encoding a 533-amino acid protein. Domain prediction

analysis revealed that CfRgs2 contains a single RGS domain and three low-complexity regions. The RGS domain consists of 136 amino acid residues, spanning positions 22 to 157 (Supplementary Figure S1A). Phylogenetic analysis demonstrated that CfRgs2 from *C. fructicola* is most closely related to its ortholog in *C. gloeosporioides*, with a bootstrap support value of 100% (Supplementary Figure S1B). This analysis supported our nomenclature, showing that CfRgs2 clusters with the expected orthologs from related species.

3.4. Generation of CfRGS2 Knockout Mutants and Complemented Strains

The knockout strategy for the *CfRGS2* gene is schematically represented in Figure 2A. Homologous recombination was employed to replace the *CfRGS2* coding region with the hygromycin resistance gene (*HPH*) cassette. Primers used for amplification and verification are indicated by numbered arrows. PCR verification using primers CfRgs2-5F/H855R and CfRgs2-7F/CfRgs2-8R confirmed the successful generation of the Δ*Cfrgs2*-1 and Δ*Cfrgs2*-2 mutant strains. The Δ*Cfrgs2*-1 and Δ*Cfrgs2*-2 are two independent knockout mutants generated to confirm that the observed phenotypes are due to the gene deletion and not a result of random off-target effects. The constructed complementation plasmid pYF11::*CfRGS2* was introduced into Δ*Cfrgs2*-1 protoplasts, yielding the complemented strain Δ*Cfrgs2/CfRGS2* (Figure 2B).

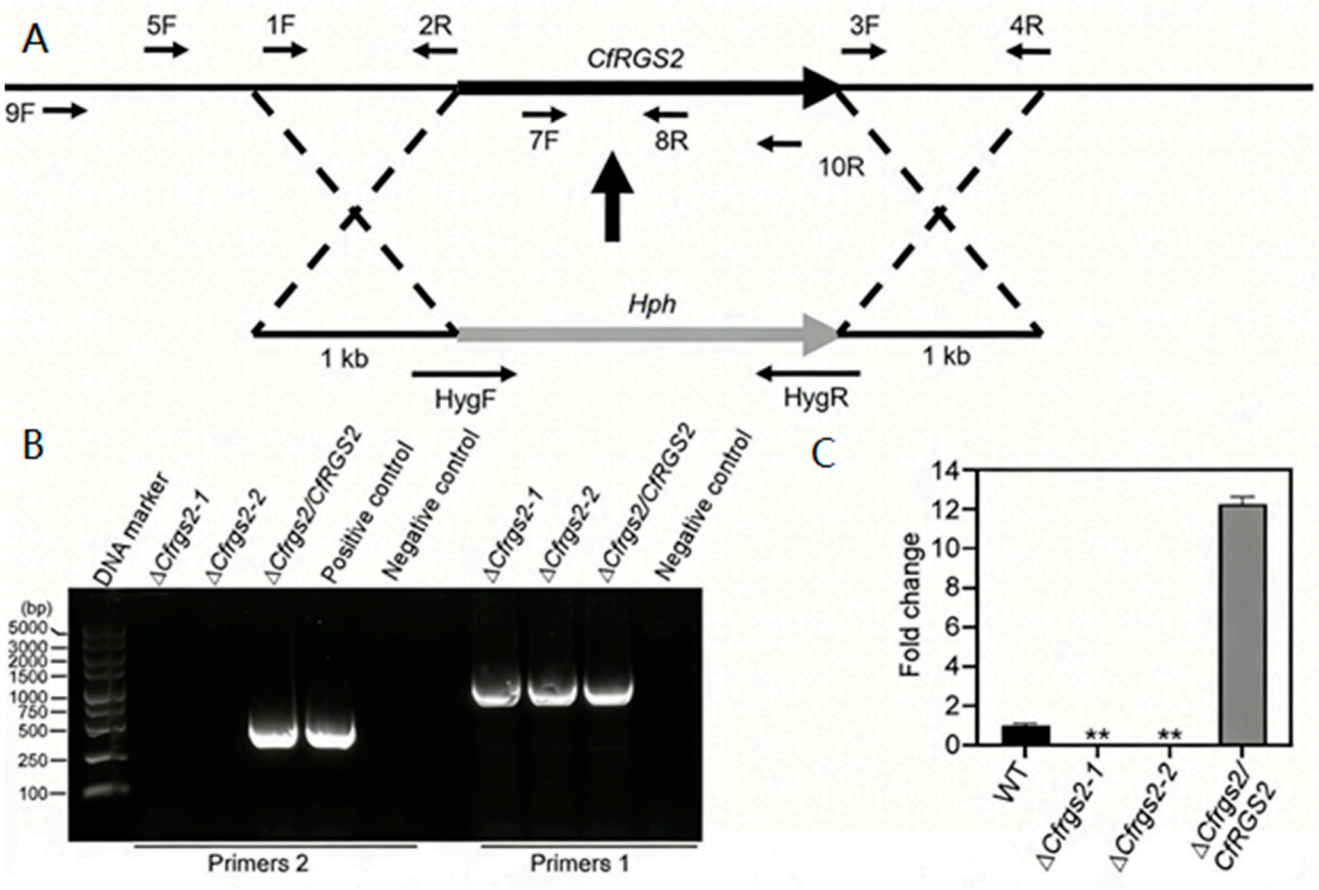

Figure 2. Generation and validation of *CfRGS2* knockout mutants and the complemented strain. (**A**): Strategy for targeted gene replacement via homologous recombination. The *CfRGS2* coding region was replaced with the *HPH* cassette. Arrows indicate primer positions. (**B**): PCR verification of WT, Δ*Cfrgs2*-1, Δ*Cfrgs2*-2, and Δ*Cfrgs2/CfRGS2* using primers 5F/H855R and 7F/8R. M: DL2000 marker. (**C**): qPCR analysis of the increased copy number of *CfRGS2*. Values represent mean ± SD ($n = 3$). ** $p < 0.01$ compared to WT.

qPCR was performed to determine the expression level of *CfRGS2* in the mutants Δ*Cfrgs2*-1 and Δ*Cfrgs2*-2, as well as in the complemented strain Δ*Cfrgs2/CfRGS2*. The results indicated that *CfRGS2* expression was increased in copy number in both the wild-type and complemented strains, whereas no expression was detected in Δ*Cfrgs2*-1 and Δ*Cfrgs2*-2, confirming the successful knockout of the target gene in the mutant (Figure 2C). However, the expression level of *CfRGS2* was significantly higher in the complemented strain, possibly due to the presence of multiple gene copies in the complementation background. The wild-type strain was used as the control, with actin serving as the reference gene.

3.5. CfRGS2 Regulates Vegetative Growth and Conidiation

Measurements of vegetative growth revealed that after a specified incubation period on PDA medium, the colony diameters of the mutants Δ*Cfrgs2*-1 and Δ*Cfrgs2*-2 reached 3.3 cm, which was significantly smaller than those of the wild-type strain (5.6 cm) and the complemented strain Δ*Cfrgs2/CfRGS2* (5.5 cm). Similarly, on minimal medium (MM), the colony diameters of both mutants were only 3.1 cm, also markedly smaller than those of the WT (4.8 cm) and the complemented strain (4.6 cm) (Figure 3A,B).

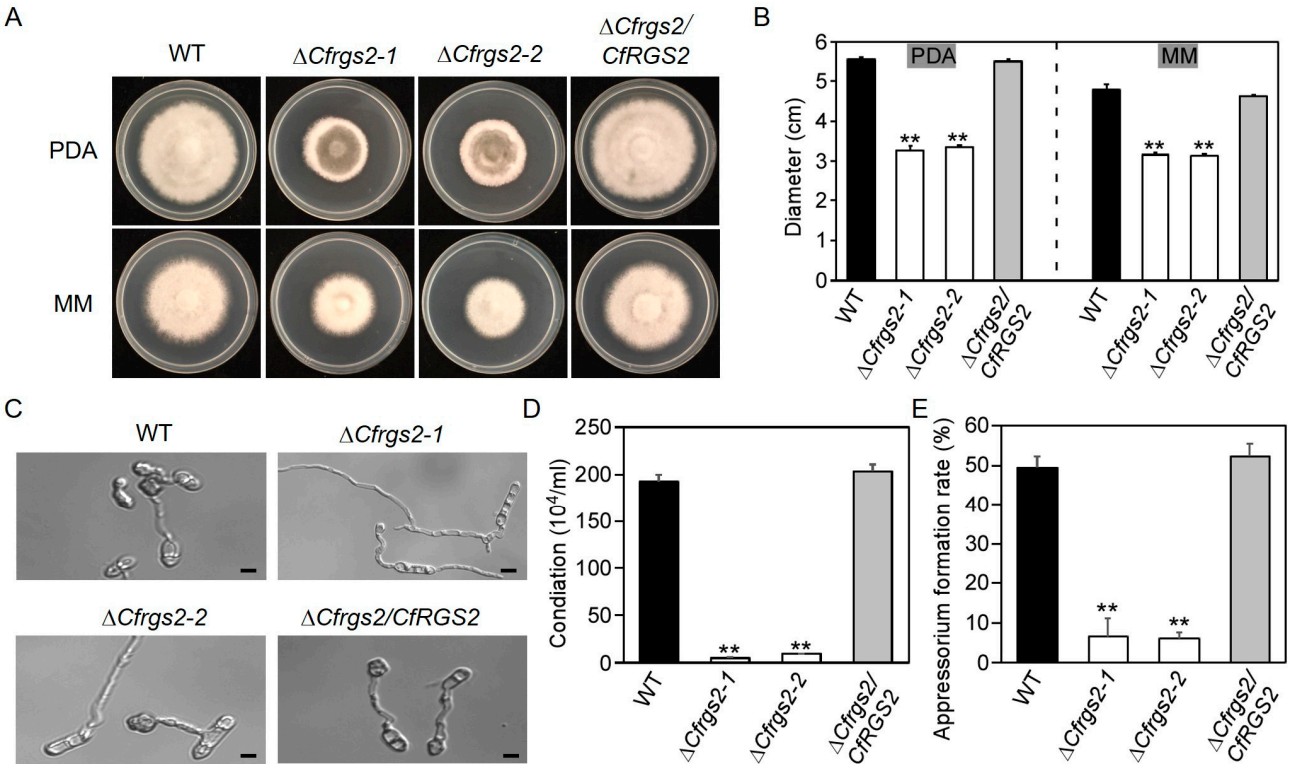

Figure 3. CfRgs2 is required for vegetative growth, conidiation, and appressorium formation. (**A**): Colony morphology of WT, Δ*Cfrgs2*-1, Δ*Cfrgs2*-2, and complemented Δ*Cfrgs2/CfRGS2* strains on PDA and MM after 3 days at 28 °C. (**B**): Colony diameters quantified from (**A**). (**C**): Microscopic images of appressorium formation on hydrophobic coverslips at 12 h post-incubation. (**D**): Conidial production of the indicated strains. (**E**): Appressorium formation rates calculated as the percentage of germinated conidia that formed appressoria. Values represent mean ± SD (n = 3). ** $p < 0.01$ compared to WT and complemented strain. Scale bar = 5 μm.

Further analysis showed that the conidiation efficiency of Δ*Cfrgs2*-1 and Δ*Cfrgs2*-2 was significantly reduced, reaching only 4% of that observed in the WT and complemented strains (Figure 3C,D, $p < 0.01$). In addition, the conidia produced by the mutants exhibited multipolar germination and abnormal morphological features, including increased germ tube branching. The appressorium formation assay revealed a severe defect in the Δ*Cfrgs2*

mutants, with only about 6% of conidia forming appressoria compared to approximately 50% in the wild-type and complemented strains (Figure 3E, $p < 0.01$). Taken together, these results indicate that *CfRGS2* plays a critical role in vegetative growth, conidium formation, and appressorium development in *C. fructicola*.

3.6. CfRGS2 Is Involved in the Response to Cell Wall Stress

To investigate the role of *CfRGS2* in responding to cell wall stress, the WT, Δ*Cfrgs2*-1 and Δ*Cfrgs2*-2, and the complemented strain Δ*Cfrgs2/CfRGS2* were cultured on PDA medium supplemented with 400 μg/mL Congo Red (CR), and the growth inhibition rates were determined. The results showed that the growth inhibition rates for Δ*Cfrgs2*-1 and Δ*Cfrgs2*-2 were 44% and 48%, respectively, which were significantly higher than those of the WT (35%) and the complemented strain (32%) (Figure 4A,B). The increased sensitivity of the mutants to CR indicates that *CfRGS2* is involved in regulating the response to cell wall stress in *C. fructicola*.

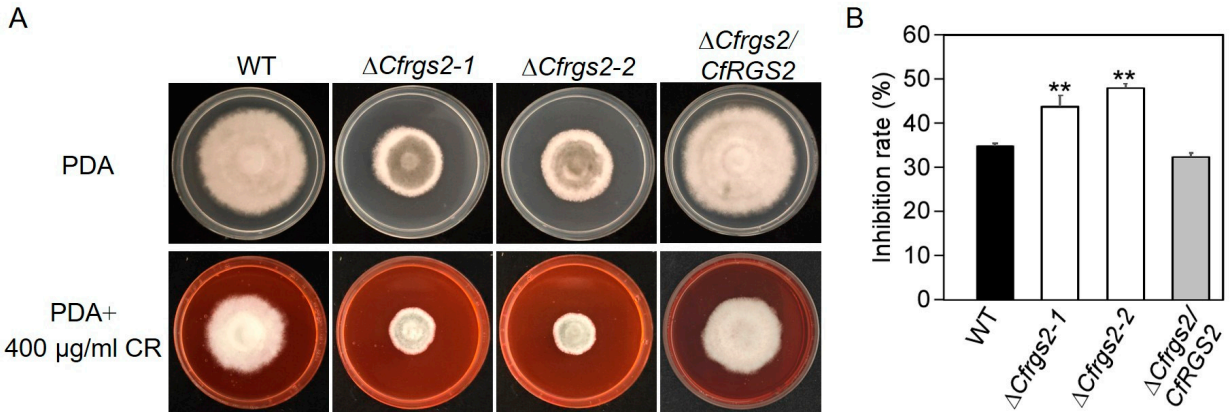

Figure 4. CfRgs2 contributes to cell wall stress tolerance in *C. fructicola*. (**A**): Colony morphology of WT, Δ*Cfrgs2*-1, Δ*Cfrgs2*-2, and the complemented strain Δ*Cfrgs2/CfRGS2* grown on PDA medium supplemented with 400 μg/mL Congo Red (CR) for 3 days at 28 °C. (**B**): Growth inhibition rates were calculated as the percentage reduction in colony diameter under CR treatment compared to control conditions. Data are presented as mean ± SD ($n = 3$). ** $p < 0.01$ indicates a statistically significant difference compared to WT and the complemented strain.

3.7. CfRGS2 Is Required for Full Pathogenicity

Pathogenicity assays were performed to evaluate the impact of *CfRGS2* deletion. Conidial suspensions of the WT, mutant strains, and the complemented strain were inoculated onto intact leaves of oil tea. The results showed that neither Δ*Cfrgs2*-1 nor Δ*Cfrgs2*-2 induced any visible lesions on unwounded leaves, whereas both the WT and complemented strains caused significant disease symptoms (Figure 5A,B; $p < 0.01$). To further examine whether the role of *CfRGS2* in pathogenicity is host-specific, we assessed the virulence of the mutants on apple fruits. The lesion areas caused by Δ*Cfrgs2*-1 and Δ*Cfrgs2*-2 were reduced by 47% and 30%, respectively, compared to the WT (Figure 5C,D), with the differences being statistically significant. In summary, these findings demonstrate that *CfRGS2* is essential for the full pathogenicity of *C. fructicola*, and its regulatory function is not limited to a specific host plant.

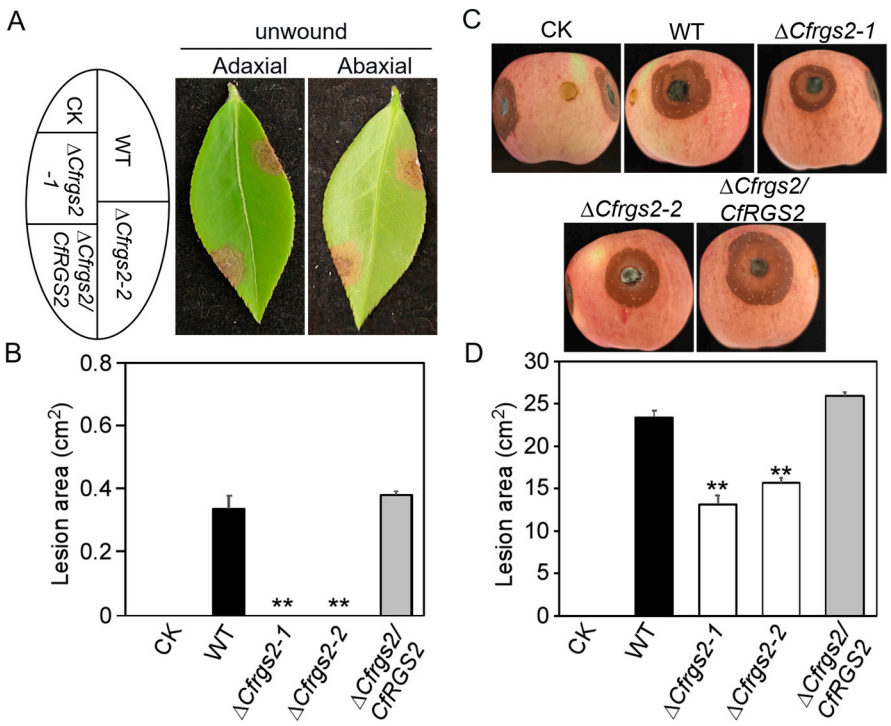

Figure 5. CfRgs2 is required for full virulence of *C. fructicola*. (**A**): Lesions on unwounded *C. oleifera* leaves 3 days post-inoculation with mycelial plugs of the indicated strains. (**B**): Quantification of lesion areas shown in (**A**). (**C**): Lesions on wounded apple fruits (cv. Fuji) 3 days post-inoculation. (**D**): Quantification of lesion diameters shown in (**C**). Values represent mean ± SD (n = 3). ** $p < 0.01$ compared to WT and complemented strain.

4. Discussion

Regulator of G protein signaling proteins are widely distributed across eukaryotes and exhibit remarkable diversity in both amino acid composition and physicochemical properties, reflecting their broad functional versatility. Despite this variability, RGS proteins typically contain a conserved RGS domain, which adopts a structure of nine α-helices that directly interacts with activated Gα-GTP, thereby accelerating the inactivation of the Gα subunit [2]. In this study, we identified seven canonical RGS proteins containing the RGS domain in *C. fructicola*. Despite having a conserved RGS domain, their distinct subcellular localization patterns suggest a potential mechanism for their functional divergence.

The G protein signaling pathway plays pivotal roles in fundamental fungal processes, including vegetative growth, sporulation, the differentiation of infection-related structures, and pathogenicity [3,6,8,9]. The functions of RGS proteins, as key regulators of this pathway, have been characterized in several phytopathogenic fungi. In *M. oryzae*, RGS proteins modulate vegetative growth, cell wall integrity, hyphal hydrophobicity, sexual/asexual sporulation, appressorium differentiation, and invasive growth [10]. In *G. zeae*, RGS proteins are implicated in diverse processes such as vegetative growth, conidiation, mycotoxin production, sexual reproduction, and virulence. Notably, FgFlbB, the homolog of CgRgs2 in *C. fructicola*, is involved in vegetative hyphal growth and influences conidial yield and morphology [6]. Similarly, in *Fusarium verticillioides*, RGS proteins regulate conidiogenesis and toxin biosynthesis [9]. Consistent with these findings, Wu et al. [16] demonstrated that CgRgs2 in *C. gloeosporioides* is critical for regulating vegetative growth, conidial production and germination, oxidative stress responses, cell wall integrity, and full pathogenicity. We identified CfRgs2 in *C. fructicola* and found that its deletion attenuates multiple pathogenic traits—including growth, sporulation, appressorium development, and virulence—phenotypes that align with those described for *CgRGS2* in *C. gloeospori-*

oides [16]. However, this functional profile diverges from that in *M. oryzae*, where *MoRGS2* is dispensable for growth and pathogenesis [10]. These comparative analyses indicate that the regulatory functions of Rgs2 are not conserved but have undergone lineage-specific evolutionary rewiring among phytopathogenic fungi.

The complemented strain Δ*Cfrgs2/CfRGS2* exhibited significantly higher CfRgs2 transcript levels than the wild-type (Figure 2C), likely due to multi-copy integration of the complementation construct during transformation. Despite this overexpression, the complemented strain fully restored all examined phenotypes to wild-type levels (Figures 3–5), confirming that the defects in Δ*Cfrgs2* mutants are specifically caused by loss of CfRgs2. The absence of phenotypic alterations beyond wild-type levels suggests tight homeostatic regulation of G-protein signaling in *C. fructicola*. Nevertheless, the multi-copy nature of complementation represents a limitation. Future generation of single-copy, site-specific integrants would enable more precise control over CfRgs2 expression and clarify potential dose-dependent effects. Western blot analysis could also determine whether increased transcript levels translate proportionally to protein levels. In summary, while CfRgs2 overexpression does not compromise our conclusion that this gene is essential for normal fungal development, it highlights the need for future studies to dissect the regulatory mechanisms maintaining signaling homeostasis in *C. fructicola*.

Previous studies on *C. fructicola* have identified multiple virulence-associated genes, including the small GTPase CfRab7, which is critical for growth, stress response, vacuole fusion, and pathogenicity [17]; the retromer component CfVps26, whose loss leads to defective conidiation, appressorium formation, glycogen metabolism, and complete loss of pathogenicity [18]; the RNA-binding protein CfNop12, which regulates development, low-temperature stress response, and virulence [19]; and epigenetic regulators such as the histone acetyltransferase CfRtt109 and deacetylase CfSnt2, both influencing growth, sporulation, and pathogenesis [20,21]. In this study, our characterization of CfRgs2 establishes it as an additional virulence factor, as its absence severely compromises pathogenic capacity. This finding contributes to the growing catalog of virulence-associated genes identified in *C. fructicola* and further underscores the complexity of the regulatory networks governing pathogenicity in this fungus.

This study provides a phenotypic characterization of CfRgs2 in *C. fructicola*, but the downstream signaling components through which CfRgs2 exerts its regulatory effects remain to be identified. RGS proteins function as GTPase-activating proteins that negatively regulate Gα subunits by accelerating GTP hydrolysis, thereby modulating downstream signaling. In other filamentous fungi, RGS proteins regulate diverse processes by targeting specific Gα subunits—for example, appressorium formation in *M. oryzae* [10] and secondary metabolism in *G. zeae* [6]. Given the pleiotropic phenotypes observed in Δ*Cfrgs2* mutants, CfRgs2 may regulate multiple Gα subunits or interact with other signaling pathways, such as cAMP-PKA or MAPK cascades. The increased sensitivity to Congo red also suggests a possible link to cell wall integrity pathways. However, the specific Gα targets of CfRgs2 and its downstream transcriptional networks remain unknown. Further studies using co-immunoprecipitation, yeast two-hybrid screening, or transcriptomic analysis will help elucidate the molecular mechanism by which CfRgs2 regulates growth, development, and pathogenicity in *C. fructicola*.

5. Conclusions

In conclusion, this study establishes that the G-protein signaling regulator CfRgs2 is a critical virulence determinant in *C. fructicola*. Targeted gene knockout revealed that CfRgs2 is indispensable for normal fungal growth, conidiation, appressorium development, and cell wall integrity. The severe attenuation of pathogenicity in Δ*Cfrgs2* mutants, evidenced by

a failure to infect unwounded hosts and significantly reduced lesion formation on wounded tissue, directly links its function to infection mechanisms. These findings demonstrate that CfRgs2 orchestrates multiple developmental and stress-responsive pathways essential to *C. fructicola* pathogenicity, providing a pivotal molecular target for future disease management strategies aimed at controlling anthracnose.

Supplementary Materials: The following supporting information can be downloaded at https://www.mdpi.com/article/10.3390/microbiolres17030053/s1. Figure S1: Phylogenetic tree and domain of CfRgs2.

Author Contributions: Conceptualization, Y.L. and H.L.; methodology, Q.H.; software, Q.H.; validation, Y.L., Q.H., and H.L.; formal analysis, Y.L.; investigation, Q.H.; resources, Y.L.; data curation, H.L.; writing—original draft preparation, Y.L.; writing—review and editing, H.L.; visualization, Q.H.; supervision, H.L.; project administration, H.L.; funding acquisition, H.L. All authors have read and agreed to the published version of the manuscript.

Funding: This study is funded by the National Key R&D Program of China (2023YFD1401301).

Institutional Review Board Statement: Not applicable.

Informed Consent Statement: Not applicable.

Data Availability Statement: The original contributions presented in this study are included in the article. Further inquiries can be directed to the corresponding author.

Conflicts of Interest: The authors declare no conflicts of interest. The funders had no role in the design of the study; in the collection, analyses, or interpretation of data; in the writing of the manuscript; or in the decision to publish the results.

Abbreviations

WT (wild-type); RGS (regulators of G-protein signaling); PCR (polymerase chain reaction); qPCR (quantitative PCR); CR (Congo red); PDA (potato dextrose agar); minimal medium (MM); ANOVA (analysis of variance).

References

1. Li, H.; Zhou, G.; Liu, J.; Xu, J. Population genetic analyses of the fungal pathogen *Colletotrichum fructicola* on tea-oil trees in China. *PLoS ONE* **2016**, *11*, e156841. [CrossRef] [PubMed]
2. Wang, Y.; Geng, Z.; Jiang, D.; Long, F.; Zhao, Y.; Su, H.; Zhang, K.; Yang, J. Characterizations and functions of regulator of G protein signaling (RGS) in fungi. *Appl. Microbiol. Biotechnol.* **2013**, *97*, 7977–7987. [CrossRef]
3. Yu, J. Heterotrimeric g protein signaling and rgss in *Aspergillus nidulans*. *J. Microbiol.* **2006**, *44*, 145–154.
4. Dohlman, H.G.; Thorner, J.W. Regulation of G protein-initiated signal transduction in yeast: Paradigms and principles. *Annu. Rev. Biochem.* **2001**, *70*, 703–754. [CrossRef]
5. Malbon, C.C. G proteins in development. *Nat. Rev. Mol. Cell Biol.* **2005**, *6*, 689–701. [CrossRef]
6. Park, A.R.; Cho, A.; Seo, J.; Min, K.; Son, H.; Lee, J.; Choi, G.J.; Kim, J.; Lee, Y. Functional analyses of regulators of G protein signaling in *Gibberella zeae*. *Fungal Genet. Biol.* **2012**, *49*, 511–520. [CrossRef]
7. Siderovski, D.P.; Willard, F.S. The GAPs, GEFs, and GDIs of heterotrimeric G-protein alpha subunits. *Int. J. Biol. Sci.* **2005**, *1*, 51–66. [CrossRef]
8. Fang, W.; Scully, L.R.; Zhang, L.; Pei, Y.; Bidochka, M.J. Implication of a regulator of G protein signalling (Bbrgs1) in conidiation and conidial thermotolerance of the insect pathogenic fungus *beauveria bassiana*. *Fems Microbiol. Lett.* **2008**, *279*, 146–156. [CrossRef]
9. Mukherjee, M.; Kim, J.; Park, Y.; Kolomiets, M.V.; Shim, W. Regulators of G-protein signalling in *Fusarium verticillioides* mediate differential host-pathogen responses on nonviable versus viable maize kernels. *Mol. Plant Pathol.* **2011**, *12*, 479–491. [CrossRef] [PubMed]
10. Zhang, H.; Tang, W.; Liu, K.; Huang, Q.; Zhang, X.; Yan, X.; Chen, Y.; Wang, J.; Qi, Z.; Wang, Z.; et al. Eight rgs and rgs-like proteins orchestrate growth, differentiation, and pathogenicity of *Magnaporthe oryzae*. *PLoS Pathog.* **2011**, *7*, e1002450. Correction in *PLoS Pathog.* **2019**, *15*, e1008187. https://doi.org/10.1371/journal.ppat.1008187. [CrossRef] [PubMed]
11. Versele, M.; de Winde, J.H.; Thevelein, J.M. A novel regulator of g protein signalling in yeast, rgs2, downregulates glucose-activation of the camp pathway through direct inhibition of gpa2. *EMBO J.* **1999**, *18*, 5577–5591. [CrossRef]

12. Zhang, S.; Guo, Y.; Li, S.; Li, H. Histone acetyltransferase Cfgcn5-mediated autophagy governs the pathogenicity of *Colletotrichum fructicola*. *mBio* **2022**, *13*, e195622. [CrossRef]
13. Altschul, S.F.; Madden, T.L.; Schaffer, A.A.; Zhang, J.; Zhang, Z.; Miller, W.; Lipman, D.J. Gapped blast and psi-blast: A new generation of protein database search programs. *Nucleic Acids Res.* **1997**, *25*, 3389–3402. [CrossRef]
14. Gao, Y.; Zhang, S.; Sheng, S.; Li, H. A *Colletotrichum fructicola* dual specificity phosphatase Cfmsg5 is regulated by the Cfap1 transcription factor during oxidative stress and promotes virulence on *Camellia oleifera*. *Virulence* **2024**, *15*, 2413851. [CrossRef]
15. Zhang, S.; Guo, Y.; Chen, S.; Li, H. The histone acetyltransferase CfGcn5 regulates growth, development, and pathogenicity in the anthracnose fungus *Colletotrichum fructicola* on the tea-Oil tree. *Front. Microbiol.* **2021**, *12*, 680415. [CrossRef]
16. Wu, M.; Li, X.; Zhang, N.; Xu, S.; Liu, Z. Gene cloning and biological function of *CgRGS2* in *Colletotrichum gloeosporioides*. *Acta Microbiol. Sin.* **2017**, *57*, 66–76.
17. Wu, Y.; Li, L.; Li, H. Function of small GTPase Rab7 in *Colletotrichum fructicola*. *Acta Microbiol. Sin.* **2022**, *62*, 2509–2520.
18. Li, X.; Zhang, S.; Li, H. Function of Vacuolar Protein Sorting CfVps26 in *Colletotrichum fructicola* on *Camellia oleifera*. *Sci. Silvae Sin.* **2021**, *57*, 94–101.
19. Yao, Q.; Li, S.; Wang, C.; Li, H. CfNop12 regulates the development, cold stress response and pathogenicity of *Colletotrichum fructicola*. *Mycosystema* **2023**, *42*, 2257–2268.
20. Wang, C.; Yao, Q.; Li, H. Function of the histone acetyltransferase Rtt109 in *Colletotrichum fructicola*, the causal organism of *Camellia oleifera* anthracnose. *Mycosystema* **2024**, *43*, 43–54.
21. Guo, Y.; Chen, Z.; Li, H.; Zhang, S. The Cfsnt2-dependent deacetylation of histone H3 mediates autophagy and pathogenicity of *Colletotrichum fructicola*. *J. Fungi* **2022**, *8*, 974. [CrossRef] [PubMed]